Mechanical Advantage of Compliant Mechanisms, Soft Robots, and Continuum Elastic Manipulators

Vishwanath Ravindran and G. K. Ananthasuresh

Abstract Only kinematics governs both motion and force transmission of rigid-body mechanisms and robots. Once contact is made with a rigid workpiece, their configuration and mechanical advantage (MA) remain fixed even when the input force increases. This is not true for compliant mechanisms, soft robots, and continuum manipulators, as their behaviour is governed by elastokinematics and their configuration evolves with changing input force. Here, the role of compliance in force transmission is investigated by appropriately delineating MA in terms of their current and past elastokinematic configurations. Furthermore, the dependence of the MA of a multi-input multi-output (MIMO) system on actuator and workpiece specifications is studied through a mathematically tractable definition of force transmission. The derived results are elucidated through a SIMO soft-pneumatic gripper and a MIMO continuum manipulator.

1 Introduction

Motion and force transmission in compliant mechanisms are governed by both kinematics and elastic deformation. This contrasts with rigid-body mechanisms and robots that rely on only kinematic considerations [1]. Functional machines in nature employ effective designs that exploit their environment and their own compliance to transmit both force and motion; examples include the muscular hydrostats in octopus arms [2] and elephant trunks [3], which exhibit remarkable force and motion transmission despite the absence

V. Ravindran
Department of Mechanical Engineering, Indian Institute of Science, Bengaluru, India

G. K. Ananthasuresh
Department of Mechanical Engineering, Indian Institute of Science, Bengaluru, India
e-mail: suresh@iisc.ac.in

of any stiff members. These have motivated the development of soft robotics systems that show similar characteristics. But research has primarily focused on recreating intended motion behavior [4], and mechanical advantage (MA) or mechanical efficiency are rarely analyzed or quantified in the literature.

Similarly, the inherent flexibility enabling compliant mechanisms has biased research toward their motion-transmission characteristics, leading to the development of several compliant systems and synthesis methods tailored to various motion-related needs. In comparison, force transmission is less understood. Force transmission is particularly crucial when designing compliant systems to interact with their surroundings or perform work on a workpiece. The development of such systems would benefit from an understanding of the dependence of force transmission on mechanism, actuator, and workpiece characteristics, which are scarce in the literature and are mostly limited to small deformations in SISO systems.

To this end, this work investigates certain practically relevant aspects of force transmission in a MIMO compliant mechanism. The paper is structured as follows: First, in Section 2, the commonly adopted notion that compliance negatively affects force transmission is investigated. Then in Section 3, mathematically tractable definitions of force transmission in MIMO systems are employed to determine the general trends in its dependence on workpiece and actuator characteristics. The trends are demonstrated through a practically motivated study on the force transmission aspects of a soft pneumatic gripper. Finally, in Section 4, the ability to manipulate force transmission through effective actuation choices in systems with more inputs than outputs is illustrated through an idealized continuum manipulator. The main takeaways are summarized in Section 5.

2 Effect of compliance on force transmission

In the seminal work on force transmission in compliant mechanisms by Salomon and Midha (1998) [5], they treated a SISO compliant mechanism as a two-output system, with a physical output port for studying force transmission and a fictitious output port associated with the mechanism's elastic deformation. Through energy-based methods, they derived the following relation:

$$\mathrm{MA} = \frac{f_o}{f_i} = \mathrm{MA}_r \left(1 - \frac{f_c}{f_i}\right), \tag{1}$$

where f_o, f_i, and f_c are the forces associated with the physical output, input, and fictitious output port, respectively, and MA_r is the MA associated with an equivalent rigid body. They suggested that the second term arising from the mechanism's compliance leads to a loss in the force-transmission capabilities of compliant bodies. This view has been commonly adopted in literature.

However, an alternative interpretation of Equation (1) is presented here to clarify the role of compliance. First, the terms in the equation can be expressed as:

$$\mathrm{MA}(f_i, u_o) = \frac{f_o}{f_i} = \left.\frac{\partial u_i}{\partial u_o}\right|_{f_i, u_o} - \frac{1}{f_i}\left.\frac{\partial \mathrm{SE}}{\partial u_o}\right|_{f_i, u_o} \equiv \mathrm{MA}_r - \mathrm{MA}_c, \tag{2}$$

where u_i, u_o are input and output displacements, and SE represents the strain energy of the mechanism at the equilibrium configuration parameterized in terms of the input force and output displacement. Then, through the Maxwell-Betti reciprocal theorem, the equation can be rewritten as:

$$\mathrm{MA}(f_i, u_o) = \frac{f_o}{f_i} = \left.\frac{\partial f_o}{\partial f_i}\right|_{f_i, u_o} - \frac{1}{f_i}\left.\frac{\partial \mathrm{SE}}{\partial u_o}\right|_{f_i, u_o} = \mathrm{iMA} - \mathrm{MA}_c, \tag{3}$$

where iMA is defined as the instantaneous mechanical advantage associated with that configuration. This suggests that MA_c is merely a difference between the instantaneous and cumulative mechanical advantage. This also explains the equivalence between the two in rigid-body mechanisms, where MA_c is identically zero; there, the kinematic configuration is frozen once the rigid workpiece is engaged. Thus, both instantaneous and cumulative mechanical advantage are the same. However, in compliant mechanisms, the mechanism's inherent compliance can accommodate, through motion/deformation, the instantaneous force transmitted from past elastokinematic configurations it has experienced before reaching its current configuration.

An illustrative example of this is a mechanical lever, replaced by a compliant beam. A schematic is presented in Fig. 1(a), where no gap is assumed with the rigid workpiece represented by the vertical roller support, the variability of the different MA terms with input force (non-dimensionalised by EI/L^2) for this mechanism is plotted in Fig. 1(b), and, the graphical interpretation of the different MA terms from the force response plot is shown in Fig. 1(c). There, from numerical computation, MA_c is observed to be negative. In this case, f_c being negative suggests that the motion/deformation of the material points in the mechanism contributes favorably to force transmission. The mechanism at that elastokinematic configuration can be imagined as a rigid-body mechanism with the same instantaneous mechanical advantage, supplemented with a predeformed spring that provides additional force. In general, it is possible for the deformation experienced by the mechanisms to be retransmitted as a force to the physical output port, thereby contributing favorably to MA.

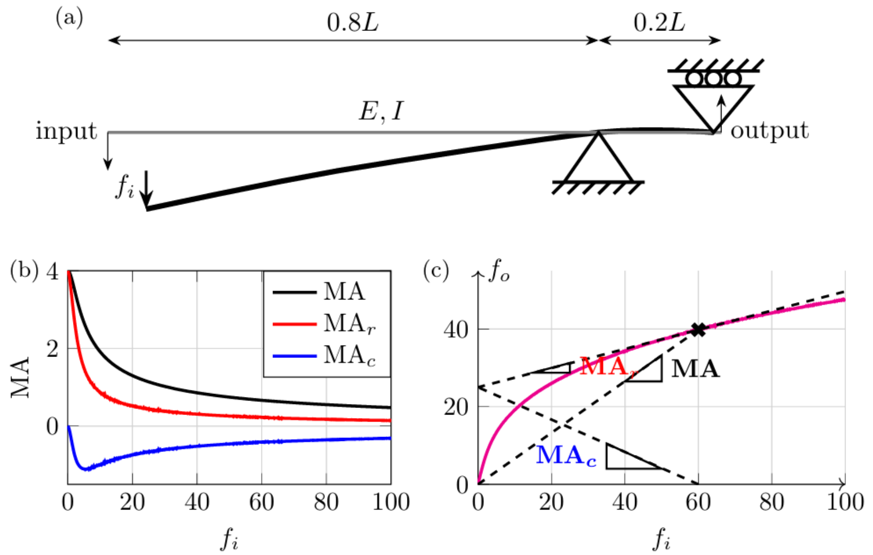

Fig. 1 A compliant mechanical lever (slenderness ratio = 100) (a) Schematic illustration (b) Variability of the different MA terms with input force (c) Variability of output force with input forces

3 Mechanical advantage of MIMO mechanisms

Most practically relevant uses of compliant mechanisms in soft robotics employ multiple input and output ports to achieve better control and functional features. In this section, some of the characteristics of force transmission noticed in SISO systems are extended to MIMO systems. In MIMO mechanisms, various performance measures for cumulative and instantaneous force transmission can be employed. Here, a root mean square-based definition is adopted for both:

$$\mathrm{MA} = \sqrt{\boldsymbol{f}_o^T \boldsymbol{D_o} \boldsymbol{f}_o} \Big/ \sqrt{\boldsymbol{f}_i^T \boldsymbol{D_i} \boldsymbol{f}_i}, \ \mathrm{iMA} = \sqrt{\boldsymbol{\Delta f}_o^T \boldsymbol{D_o} \boldsymbol{\Delta f}_o} \Big/ \sqrt{\boldsymbol{\Delta f}_i^T \boldsymbol{D_i} \boldsymbol{\Delta f}_i} \tag{4}$$

where $\boldsymbol{D_o}$ and $\boldsymbol{D_i}$ are diagonal matrices providing normalized weights, i, o, and f refer to the input, output, and non-loaded degree of freedom.

For small deformation (or system linearized at an arbitrary equilibrium configuration), the static deformation characteristics can be represented through the initial compliance matrix:

$$\begin{Bmatrix} \boldsymbol{u}_i \\ \boldsymbol{u}_o \\ \boldsymbol{u}_f \end{Bmatrix} = \begin{bmatrix} \boldsymbol{C}_{ii} & \boldsymbol{C}_{io} & \boldsymbol{C}_{if} \\ \boldsymbol{C}_{oi} & \boldsymbol{C}_{oo} & \boldsymbol{C}_{of} \\ \boldsymbol{C}_{fi} & \boldsymbol{C}_{fo} & \boldsymbol{C}_{ff} \end{bmatrix} \begin{Bmatrix} \boldsymbol{f}_i \\ \boldsymbol{f}_o \\ \cancelto{\mathbf{0}}{\boldsymbol{f}_f} \end{Bmatrix} \tag{5}$$

Then, MA can be written as:

$$\mathrm{MA} = \sqrt{\left(\boldsymbol{f}_i^T \boldsymbol{A_1} \boldsymbol{f}_i - 2\boldsymbol{f}_i^T \boldsymbol{A_2} \boldsymbol{u}_o + \boldsymbol{u}_o^T \boldsymbol{A_3} \boldsymbol{u}_o\right) \Big/ \left(\boldsymbol{f}_i^T \boldsymbol{D_i} \boldsymbol{f}_i\right)}, \tag{6}$$

where $\boldsymbol{A_1} = \boldsymbol{C}_{io}\boldsymbol{C}_{oo}^{-1}\boldsymbol{D_o}\boldsymbol{C}_{oo}^{-1}\boldsymbol{C}_{oi}$, $\boldsymbol{A_2} = \boldsymbol{C}_{io}\boldsymbol{C}_{oo}^{-1}\boldsymbol{D_o}\boldsymbol{C}_{oo}^{-1}$, and $\boldsymbol{A_3} = \boldsymbol{C}_{oo}^{-1}\boldsymbol{D_o}\boldsymbol{C}_{oo}^{-1}$. With this relation, the dependence of MA on actuator and workpiece specifications can be studied.

Suppose output displacements (gap) $\boldsymbol{u}_o = \boldsymbol{u}_o^{\boldsymbol{g}}$ are prescribed, and they could be just realized at a corresponding input load of $\boldsymbol{f}_i^{\boldsymbol{g}}$. Then, if $\boldsymbol{f}_i - \boldsymbol{f}_i^{\boldsymbol{g}}$ is assumed to scale with a parameter s as $s\boldsymbol{f}_i^{\boldsymbol{g}}$, then MA can be posed as:

$$\mathrm{MA}_1(\boldsymbol{f}_i) = \sqrt{\frac{(\boldsymbol{f}_i - \boldsymbol{f}_i^{\boldsymbol{g}})^T \boldsymbol{A_1} (\boldsymbol{f}_i - \boldsymbol{f}_i^{\boldsymbol{g}})}{\boldsymbol{f}_i^T \boldsymbol{D_i} \boldsymbol{f}_i}},\ \mathrm{MA}_1(s) = \frac{s}{1+s}\alpha, \quad (\text{for } s \geq 0) \tag{7}$$

where α is a nonnegative quantity representing the MA of the structure (when $\boldsymbol{u}_o = \mathbf{0}$). Here, we note that they follow a rectangular hyperbola similar to what is expected in SISO mechanisms [6].

Similarly for a specified input force $\boldsymbol{f}_i^{\boldsymbol{g}}$ associated with a corresponding output displacement (gap) of $\boldsymbol{u}_o^{\boldsymbol{g}}$. If $\boldsymbol{u}_o - \boldsymbol{u}_o^{\boldsymbol{g}}$ is assumed to scale as $s\boldsymbol{u}_o^{\boldsymbol{g}}$, then:

$$\mathrm{MA}_2(\boldsymbol{u}_o) = \sqrt{\frac{(\boldsymbol{u}_o^{\boldsymbol{g}} - \boldsymbol{u}_o)^T \boldsymbol{A_3} (\boldsymbol{u}_o^{\boldsymbol{g}} - \boldsymbol{u}_o)}{\boldsymbol{f}_i^{\boldsymbol{g}\ T} \boldsymbol{D}_i \boldsymbol{f}_i^{\boldsymbol{g}}}},\ \mathrm{MA}_2(s) = -s\alpha \quad (\text{for } s \leq 0) \tag{8}$$

Here, MA follows a negatively sloped line along s with a constant y-intercept (α) for varying $\boldsymbol{f}_i^{\boldsymbol{g}}$, similar to what is noted in SISO mechanisms.

In the case of a compliant workpiece being adhered to the mechanism, the MA can be posed as

$$\mathrm{MA}(\boldsymbol{K_w}) = \sqrt{(\boldsymbol{K_w}\boldsymbol{u}_o)^T \boldsymbol{D_o} (\boldsymbol{K_w}\boldsymbol{u}_o)} \Big/ \sqrt{\boldsymbol{f}_i^T \boldsymbol{D_i} \boldsymbol{f}_i} \tag{9}$$

where $\boldsymbol{K_w}$ is a positive semi-definite diagonal matrix encoding the stiffness of the compliant workpiece at the corresponding output DoF. To understand functional variation with this stiffness matrix, we will assume $\boldsymbol{K_w} = k_w\boldsymbol{I}$. In this case, MA can be expressed as:

$$\mathrm{MA}(k_w) = \sqrt{\boldsymbol{f}_i^T \boldsymbol{C}_{io} (\frac{1}{k_w}\boldsymbol{I} + \boldsymbol{C}_{oo})^{-1} \boldsymbol{D_o} (\frac{1}{k_w}\boldsymbol{I} + \boldsymbol{C}_{oo})^{-1} \boldsymbol{C}_{oi} \boldsymbol{f}_i} \Big/ \sqrt{\boldsymbol{f}_i^T \boldsymbol{D_i} \boldsymbol{f}_i} \tag{10}$$

It can be noticed that as k_w tends to zero, MA becomes zero, and in the case where k_w tends to infinity, the MA saturates to a constant value (α), identical to that of the structure.

In most practical applications, these behaviors cannot be expected to obey exactly, as specifications cannot be presented in this idealized manner and due to large deformation effects. However, the overall characteristics can show similar dependence to a meaningful extent. To assert this, the example of the soft pneumatic bellow-based gripper presented in Figs. 2(a) and 2(b) can be considered. Here, the points on the gripper's end surface represent the output, while those on the cavity's surface represent the input. By employing suitable forms of $\boldsymbol{D_i}$ and $\boldsymbol{D_o}$, the MA can be posed as:

$$\mathrm{MA} = \sqrt{\int_{\partial\Omega_o} p^2 \, \mathrm{d}A} \Bigg/ \left(p_i \sqrt{\int_{\partial\Omega_o} \mathrm{d}A} \right) \tag{11}$$

In this problem, the workpiece specifications cannot be prescribed in a mathematically tractable manner, the mechanism undergoes significant deformation to engage and transmit forces, and it also exhibits contact nonlinearity. Despite these critical details, the overall variation of MA with the actuator and workpiece specifications shows behavior similar to the idealized relations derived earlier, as shown in Figs. 2(c), 2(d), and 2(d) (linear elastic properties with $E = 1$ MPa and $\nu = 0.45$ are assumed, the principal strain in the simulations are not large enough (<0.6) to warrant the need for more sophisticated material models). In the first figure, there are some strong fluctuations due to the way the gripper engages the rigid workpiece in certain configurations, but overall, the response appears similar to a rectangular hyperbola. In the MA_2 plots, a linear decline with a negative slope and similar y-intercepts is observed. And as shown in Fig. 2(e), for a fixed input pressure and workpiece gap, as workpiece stiffness (controlled by the workpiece's Young's modulus) increases, the MA value saturates. Additionally, it is worth noting that the MA value for the specifications studied here is very poor. Here, the results suggest that a significant portion of the applied work is lost to deformation of the mechanism.

4 Optimal actuation and effect of pose on force transmission

One particular advantage of the definition employed in Equation (4) is that it allows for the immediate computation of the upper and lower bounds of iMA for all possible incremental input loads. By incorporating the elastokinematics, the iMA can be computed as:

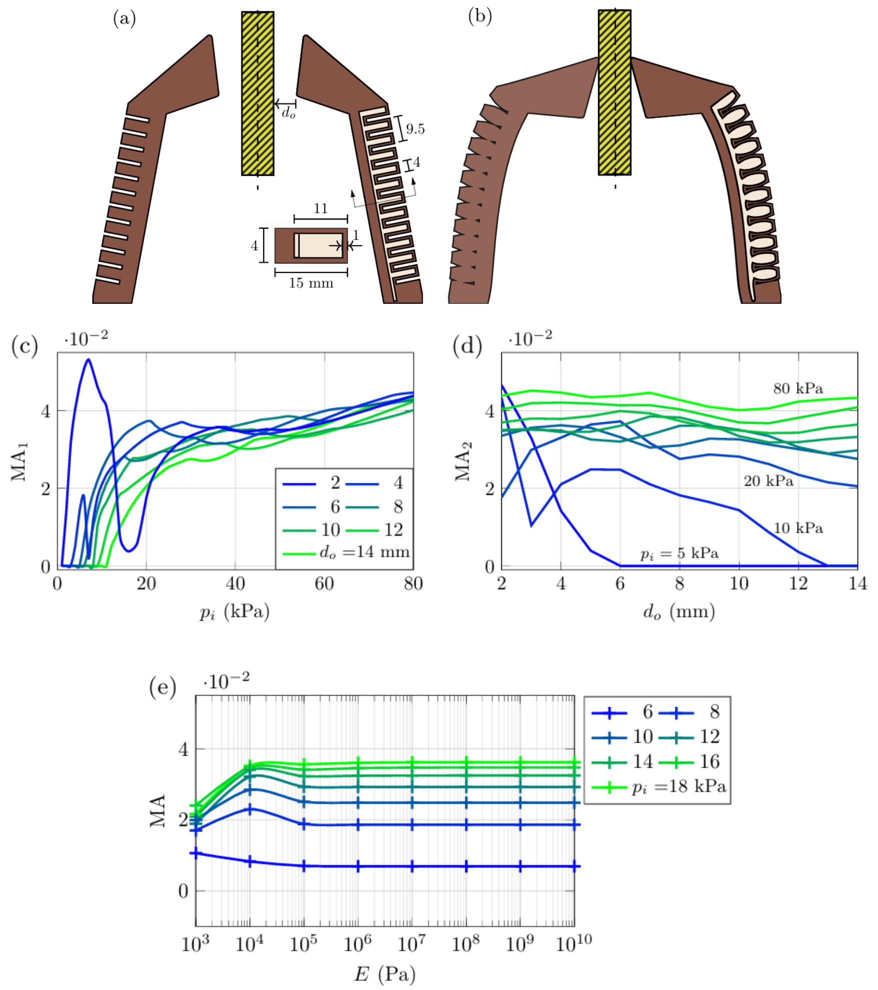

Fig. 2 Force transmission characteristics of a soft-pneumatic gripper (a) Schematic and dimensions (b) Deformed configuration corresponding to $p_i = 80$ kPa, $d_o = 9$ mm (c) Variability of MA with input pressure for a fixed workpiece gap (d) Variability of MA with workpiece gap for a fixed input pressure (e) Variability of MA with workpiece stiffness for fixed input force and workpiece gap ($d_o = 6$ mm)

$$\mathrm{iMA}(\boldsymbol{\Delta f}_i) = \sqrt{(\boldsymbol{\Delta f}_i)^T \boldsymbol{B}_1 (\boldsymbol{\Delta f}_i)} \Big/ \sqrt{(\boldsymbol{\Delta f}_i)^T \boldsymbol{D_i} (\boldsymbol{\Delta f}_i)}, \tag{12}$$

where $\boldsymbol{B}_1 = \boldsymbol{C_{io}} \boldsymbol{C_{oo}^{-1}} \boldsymbol{D_o} \boldsymbol{C_{oo}^{-1}} \boldsymbol{C_{oi}}$ and $\boldsymbol{C}\left(\boldsymbol{f}(\boldsymbol{u})\right)$ here refers to the tangent compliance matrix at the instantaneous configuration. In which case, the maximum realizable by the incremental input loads can be computed by identifying the eigenvalues of the following eigenvalue problem:

$$\sqrt{\boldsymbol{D_o}}\boldsymbol{C}_{oo}^{-1}\boldsymbol{C}_{oi}\boldsymbol{f}_i = \lambda\sqrt{\boldsymbol{D_i}}\boldsymbol{f}_i, \tag{13}$$

where the maximum iMA (iMA*) is given by the largest eigenvalue.

From Equation (12), it can be observed that iMA depends on two aspects: incremental input loads and the elastokinematic configuration. Now, by considering only the iMA*, the dependence of the elastokinematic configuration on the maximum realizable iMA can be studied. In Figure 3, the effect of the pose of a continuum arm on the incremental mechanical advantage after contact with a rigid workpiece is studied. This continuum arm (illustrated in Fig. 3(a)) is inspired by muscular hydrostats such as octopus arms. Where, through appropriate actuation of muscles along the arm, they generate moments that drive the arm's motion. Here, flexural rigidity is assumed to vary linearly from $10EI$ at the fixed end to EI at the tip. And the iMA for this problem is posed as:

$$\text{iMA} = \left(\sqrt{\Delta f_{t,x}^2 + \Delta f_{t,y}^2}\right) \Big/ \left(\sqrt{\Sigma_{i=2}^{t-1} \Delta M_i^2}\right), \tag{14}$$

where the indexes refer to the node numbers, numbered starting from the fixed end till tip (t). The effect of two different poses on the instantaneous force transmission and the distribution (along undeformed length) of the respective input moment applied to reach that configuration ($\boldsymbol{M^*}$), along with the optimal incremental moment ($\boldsymbol{\Delta M^*}$), is shown in Figs. 3(b) and 3(c). Here, the iMA* of the second pose is almost thrice that of the first. This example illustrates the potential to favorably alter force transmission characteristics by appropriately evolving the elastokinematic configuration through motion control.

5 Conclusion

As both force and motion are integral expectations from any machine architecture, an improved understanding of them would aid in the design of more functional soft robots or compliant systems. Motivated by these broad objectives, this paper discusses certain practically relevant aspects of force transmission in compliant mechanisms. The main takeaways from this work are summarized:

1. The mechanical advantage of SISO mechanisms can be decomposed into terms representing instantaneous force transmission and cumulative motion of the entire mechanism due to deformation, which can aid in diagnosing their performance. And, interestingly, in certain cases, the energy "lost" during the mechanism's deformation can enable favorable force transmission.

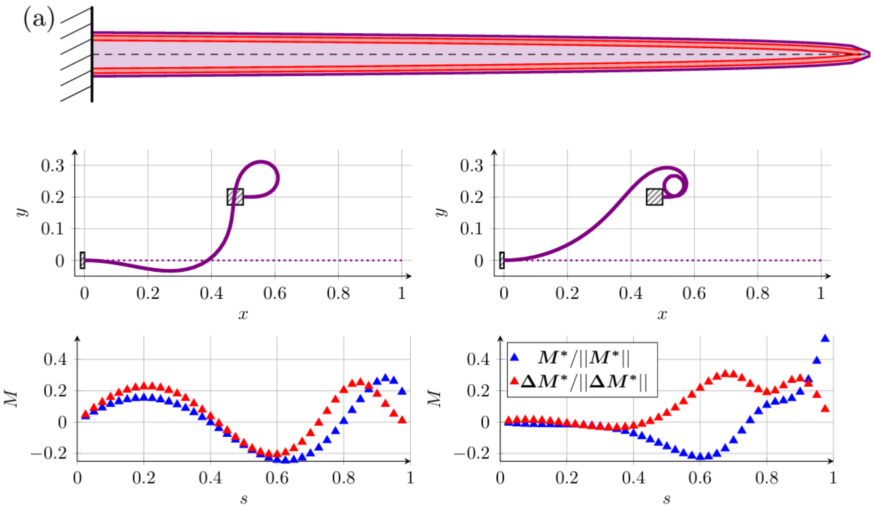

(b) Pose-1 (iMA* = 11.74)   (c) Pose-2 (iMA* = 30.20)

Fig. 3 Effect of pose on force transmission (a) An idealized continuum arm

2. For small deformation, under an appropriate definition of performance measures, force transmission in MIMO systems shows dependence on actuator and workpiece specifications, qualitatively similar to SISO systems.
3. In compliant systems with more inputs than outputs, by appropriately controlling poses, desirable force transmission characteristics can be achieved.

References

1. Erdman, A.G., Sandor, G.N.: Mechanism Design: Analysis and Synthesis. Vol. 1. Prentice-Hall International, Englewood Cliffs (1997)
2. Kennedy, E.B.L. et al.: Octopus arms exhibit exceptional flexibility. Sci. Rep. 10, 20872 (2020)
3. Olson, W. et al.: Elephant trunks: strength and dexterity from mini-fascicles. Curr. Biol. 33(22), R1203R1205 (2023)
4. Wang, Z. et al.: SpiRobs: logarithmic spiral-shaped robots for versatile grasping across scales. Device 3(4), 100646 (2025)
5. Salamon, B.A., Midha, A.: An introduction to mechanical advantage in compliant mechanisms. *J. Mech. Des.* **120**(2), 311–315 (1998)
6. Dixit, S., Ananthasuresh, G.K.: Revisiting mechanical advantage of compliant mechanisms. Proc. ASME IDETC/CIE (MR) (2023)